Microsphere Resonators for Biodetection

L. Echeveria*, S. Gilmore*, B. Demory*, C. Tolfa*, S. Harrison*, G. Chavez*, A. Chang*, P. Singh* and T. Bond*

*Lawrence Livermore National Laboratory, Livermore, CA, USA

ABSTRACT

Whispering Gallery Mode microresonators are suitable for biosensing applications as they exhibit large Quality factors (Q) capable of sensing single nanoparticles, while also showcasing a dramatically reduced footprint compared to standard optical sensing techniques. The presence of a biological analyte on the microresonator's surface results in a small change in the resonator's overall diameter and refractive index. This induces a shift in resonant properties such as the center wavelength, the linewidth, and the amplitude, which can be measured in real time. In this paper we will discuss details of our optical sensing technique. We describe our microsphere and tapered fiber fabrication processes, we provide evidence of an effective biofunctionalization procedure, and we present spectral data from real-time biosensing.

Keywords: microspheres, optical sensor, biosensing

1 INTRODUCTION

In the last several decades, researchers have allocated an increasing amount of resources towards studying biochemical sensing techniques [1]. This trend is likely due to the wide range of applications biosensing technology provides. Deployable biosensors that are accurate and reliable could lead to breakthroughs in studies that include biosecurity, aerosol virus transmission, and environmental restoration, to name a few.

With proper biosensing capabilities, biodegradation and bioremediation are two such phenomena that can be exploited for a variety of applications. Biodegradation involves decomposition by microorganisms and bioremediation occurs when similar species are used to restore the environment. For example, certain microorganisms have been shown to be able to remove hazardous wastes and pollutants, such as mercury and petroleum products, from the environment [2].

Optical sensing techniques provide many advantages suitable for biosensing. These features include an increased level of sensitivity and response time while also having a reduced device footprint compared to other biosensors [3]. Optical cavities that support Whispering Gallery Modes (WGM) can vastly reduce the size, weight, and power, typically used in optical sensing mechanisms, and can be used for other applications including gas sensing [4] and fluidic sensing [5]. WGM microresonators used in this research exhibit large Quality (Q) factors [6] with extremely narrow resonant linewidths. Consequently, these resonators provide a light-matter interaction length on the order of centimeters, allowing for sensitive detection in the surrounding environment. The resonant properties of a WGM microresonator are dependent upon the resonator's physical geometry, including diameter, eccentricity, index of refraction, and so on. Thus, the presence of a biomolecule on the resonator's surface will result in a small change in these physical specifications. This is measurable by characterizing the amplitude, free spectral range, or linewidth shift of the resonance spectra.

2 OPTICAL SENSING

2.1 Methodology

Our optical sensor consists of two major components – a tapered optical fiber and a microsphere. The latter of the two components acts as our microresonator. The former is a fiber that is tapered down to a small waist diameter such that light can escape from the core and an evanescent field is created when connected to an infrared laser source. The microsphere is coupled into the evanescent field while the probe scans between a lower and upper bounded wavelength to produce a transmission spectrum seen in figure 1. Sudden dips in the transmission occur at resonant wavelengths due to total internal reflection of light within the cavity.

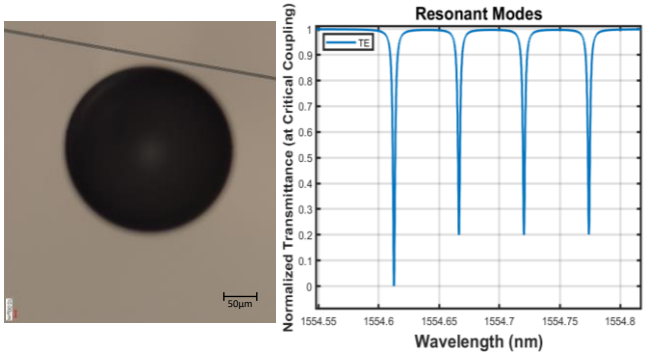

Figure 1: Microscope image of the coupling scheme with a tapered fiber atop of a microsphere (left). Theoretical transmission of a coupled system (right).

2.2 Fabrication

Both components of the optical sensor are fabricated from SMF-28 fiber. Sphere fabrication is fairly straightforward and mimics the fabrication of a ball lens. First the coating must be stripped off of the end of a ~6cm length of fiber. Once the cladding of the fiber is exposed, the tip of the fiber is cleaved and then cleaned with isopropanol. The prepped fiber is loaded into our Fitel S179 fusion splicer where the tip is repeatedly melted with ARC pulses until the desired sphere diameter is met. Typically we fabricate spheres with a diameter of 250µm. Spheres with this target diameter are advantageous due to their simplicity to mass fabricate, which allows for a straightforward testing of biofunctionalization. Smaller spheres can be fabricated by tapering the starting stalk diameter [4].

Fabrication of the tapered fiber is more complex. The diameter of our fiber with the coating removed is 125µm. Fusion splicing techniques can be applied to reliably create a parabolic taper with a waist diameter of 20µm. Finally, the fiber is treated with a hydrofluoric (HF) wet chemical etching process to achieve our final waist diameter of <5µm [4].

3 BIOFUNCTIONALIZATION

3.1 Methodology

Biofunctionalization is a process whose goal is to bind or conjugate different bioorganisms onto the surface of our spheres while limiting nonspecific binding. The effectiveness of this procedure is crucial to the overall performance of the sensor. As discussed previously, the sensor's narrow sensitivity comes from the resonator's high Q factor. However, the specificity of the sensor comes as a result of the biofunctionalization process.

Our biofunctionalization procedure adopts an antibody/antigen surface sensing scheme to ensure high selectivity of our analyte. Figure 2 shows a pictorial representation of our three step biofunctionalization procedure. The process starts with a Silane-PEG1K-NHS ester deposition. Spheres are immersed in a solution containing 5mg Silane-PEG-NHS (purchased from Biochempeg), 20ml toluene (Sigma-Aldrich), and 100µl methanol (Sigma-Aldrich) at 60°C for one hour. This step results in a thin film (~2nm) uniformly coated on the surface of the microsphere with an NHS group that is functional with our immobilized antibodies (Bio-Rad). The proceeding step immerses the microsphere in a solution containing 94.4% phosphate buffered saline (PBS), 0.6% sodium bicarbonate, and 5% antibody solution. The antibodies on the microsphere surface now act as receptors for the bioorganism being used. Finally, we incubate the microsphere for 2 hours in a solution containing the analyte. Microspheres are rinsed in PBS post-conjugation to wash any nonspecifically bound antigens.

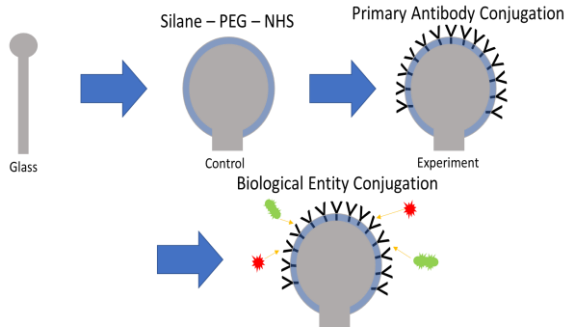

Figure 2: Pictorial representation of the steps used to functionalize the surface of a microsphere with bioorganisms.

3.2 Testing

We investigated the effectiveness of the biofunctionalization procedure by testing with a virus group and bacteria group. For the virus group we use Influenza A (Charles River) and for the bacteria group we use Escherichia Coli K-12 (E. Coli, cultured in house). Both species are inactivated before use. In order to monitor conjugation rates properly, the bioorganisms are fluorescently tagged with a DiO cell-labeling solution prior to use.

To test for conjugation we separate microspheres into a +antibody (+ab) group and a -antibody (-ab) group. Spheres in the +ab group go through the functionalization process as previously described. Spheres in the -ab group are treated with a solution containing 90% PBS and 10% 1M Trizma in replacement of the antibody solution. This hydrolyzes the NHS ester which should immobilize any antigen binding to the sphere. Both groups go on to receive treatment with the bioorganism, the only difference is the presence of antibodies, or lack thereof. Having a direct comparison of the +ab group and -ab group is beneficial to test for nonspecific binding. In the ideal case, one would see high conjugation rates when antibodies are present and low conjugation rates when antibodies are absent.

Our results, shown in figure 3, analyze conjugation rates using two separate methods. For the E. Coli experiment, we quantify conjugation rates by examining the fluorescent intensity of the microspheres. Individual bacteria cells are difficult to count manually, so this procedure analyzes the fluorescent intensity of the tagged cells. The +ab group has an average pixel intensity of 10.54 per sphere and the -ab group has an average intensity of 2.79 per sphere. For the Influenza A experiment, we quantify conjugation rates by manually counting the number of cells bound to the spheres. The +ab group has an average of 21.17 cells per sphere and the -ab group has no visible cells on the sphere surface. Both of these results yielded statistical significance when analyzed with a p-test.

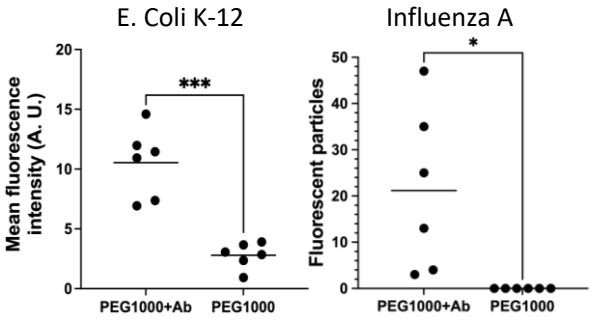

Figure 3: +Antibody and -Antibody group performance using E. Coli (left) and Influenza A (right).

4 OPTICAL MEASUREMENTS

4.1 Microfluidic Cell

Real-time optical measurements during the functionalization process requires both the tapered fiber and microsphere to be fully submerged in an aqueous environment. In our previous work, we took measurements in air after each step of functionalization. We found that doing so adds many non-idealities to the sphere surface, resulting in a full order of magnitude drop in Q factor by the final measurement [7]. Devising a method for measurements in an aqueous environment avoids excessive microsphere handling and enables real-time analysis during functionalization.

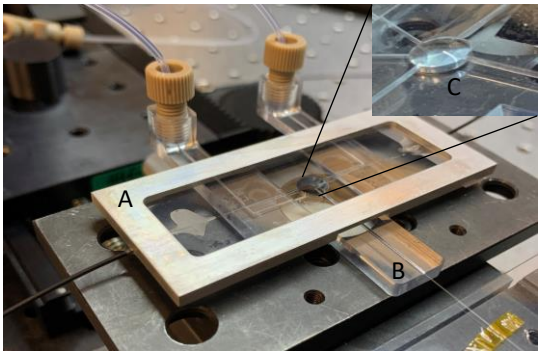

Figure 4: Image of our microfluidic cell. Included in the image are the tapered fiber glued to a glass frame (A), the microsphere in its channel (B) and the well filled to a meniscus (C).

To accomplish this scenario we designed a microfluidic cell customized to have compatibility with our coupling scheme. Pictured in figure 4, the cell contains many complementary features to house our optical setup. First, the top surface contains orthogonal channels for the tapered fiber and microsphere to lay. The microsphere, usually controlled by a micro-piezo controller, rests in a channel of slightly greater depth compared to the taper channel to allow for both top coupling and bottom coupling. The coupled system is located in the top plane of a cylindrical well of approximately 85µl in volume. Two tunnels feed into the bottom of the well, one used for infusion of solution and one used for withdrawal. Mechanical syringe pumps are used to administer flow rates of solutions. Infusion of a solution fills the well with surface tension working in our favor to create a meniscus that encapsulates our coupled system in an aqueous environment.

4.2 Environmental Sensing

The performance of our real-time measurement system was investigated through a series of fluidic tests. Altering the index of refraction around the coupled system will result in either a red shift or blue shift of resonant wavelength location depending on if the index is increased or decreased, respectively. Our initial tests evaluated the resonance stability in phosphate buffered saline (PBS) and Millipore water. In this experiment, we first couple the system under a meniscus of PBS and then simultaneously infuse and withdraw PBS at a rate of 200µl/min. After measuring the resonance data for 2 hours, we switch our solution to Millipore water and continue to measure the response. Using the Sellmeier equation, we conclude that at 1555nm, PBS has a refractive index of n = 1.318 and water has a refractive index of n = 1.315 for a total $\Delta n = 0.003$ [8]. Using Lumerical FDTD, we simulated the electric field intensity inside the sphere while submerged in both PBS and water. Simulated results found a total shift of $\Delta\lambda$ = ~35pm at peaks near 1555nm. Our measurements verify this result by monitoring the transmission at the output of the coupled system and seeing a 30pm resonance blue shift when transitioning from PBS to water.

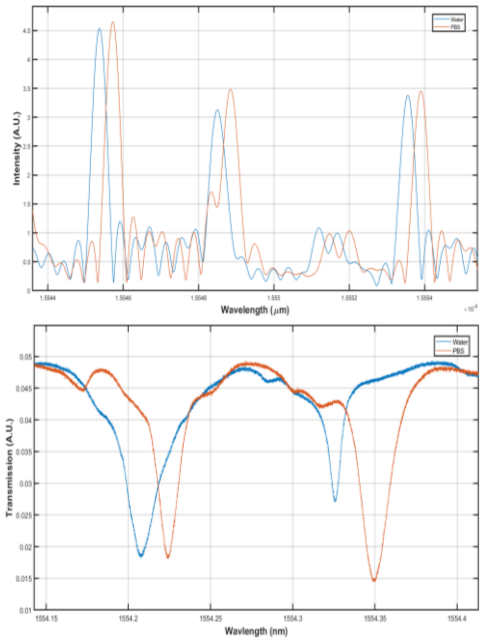

Figure 5: Simulated peaks in PBS and water (top). Experimental data of transmission vs wavelength in PBS and water (bottom).

To expand upon initial tests, we conducted another study in which we mixed various concentrations of PBS and water while infusing into the cell. The data from this experiment, shown in figure 6, suggest that we are able to detect even smaller index changes than the initial $\Delta n = 0.003$. Modeling our data with a linear regression fit shows a total peak shift of 32.7pm.

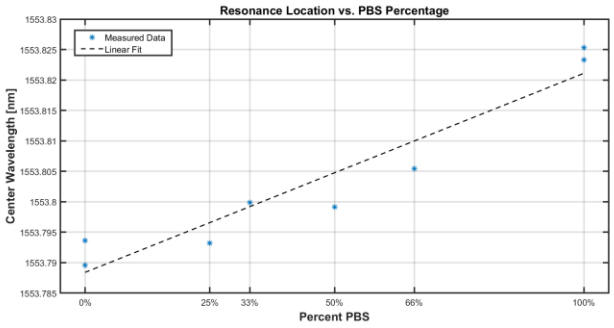

Figure 6: Resonance wavelength location vs. percent PBS concentration.

4.3 Biosensing

The data in figure 5 suggests that not only can we optically sense minute refractive changes in an aqueous solution, but we also have stability to a few picometers over long periods of time. To measure shifts due to conjugation of bioorganisms, we measure resonances before, during, and after functionalization. Initial and final measurements are taken in sterile PBS. Measurements taken during functionalization are done by flowing a set bioorganism concentration into the microfluidic well. For E. Coli we inject a concentration of ~10,000 CFU/ml and for influenza we inject a concentration of 0.1mg/ml.

Our initial results show a ~15pm blue shift due to adsorption of E. Coli. This is an unexpected result, as we anticipate a shift in the red direction. Using the approximation of $\Delta\lambda/\lambda = \Delta R/R + \Delta n/n$, where λ is the resonance location, R is the sphere radius, and n is the medium index, we expect that positive changes to the radius and index will result in a positive (red) shift in resonance location [9]. Our future work will investigate the validity of our initial measurements. We are able to verify conjugation with our E. Coli sample by fluorescently imaging the sphere post-conjugation. However, some other factors are contributing to the system causing an obliteration of the real response. Blue shifting may be occurring due to thermal contraction of the sphere [10], pressure effects induced by the continuous flow of solutions, or other thermo-optic effects.

LLNL-CONF-826098

THIS WORK WAS PERFORMED UNDER THE AUSPICES OF THE U.S. DEPARTMENT OF ENERGY BY LAWRENCE LIVERMORE NATIONAL LABORATORY UNDER CONTRACT DE-AC52-07NA27344. LAWRENCE LIVERMORE NATIONAL SECURITY, LLC

REFERENCES

[1] González-Rodríguez, Jose & Raveendran, Mukhil. (2015). Importance of Biosensors. Biosensors Journal. 04. 10.4172/2090-4967.1000e104.

[2] Abdolahi, Ahmad & Hamzah, Esah & Ibrahim, Zaharah & Hashim, Shahrir. (2014). Microbially influenced corrosion of steels by Pseudomonas aeruginosa. CORROSION REVIEWS. 10.1515/corrrev-2013-0047.

[3] Soria S, Berneschi S, Brenci M, Cosi F, Nunzi Conti G, Pelli S, Righini GC. Optical Microspherical Resonators for Biomedical Sensing. Sensors. 2011; 11(1):785-805.

[4] B. J. Demory, S. Harrison, C. Tolfa, L. T. Echeveria, P. K. Singh, V. V. Khitrov, K. G. Heinz, A. S.-P. Chang, T. Bond, "Progress on optical microspheres for CO2 sensors," Proc. SPIE 11672, Laser Resonators, Microresonators, and Beam Control XXIII, 116720R (5 March 2021);

[5] L. Labrador-Páez, K. Soler-Carracedo, M. Hernández-Rodríguez, I. Martín, T. Carmon, and L. Martin, "Liquid whispering-gallery-mode resonator as a humidity sensor," Opt. Express 25, 1165-1172 (2017).

[6] Righini, G.C., Dumeige, Y., Féron, P. et al. Whispering gallery mode microresonators: Fundamentals and applications. Riv. Nuovo Cim. 34, 435–488 (2011).

[7] Logan Echeveria, Sean Gilmore, Sara Harrison, Ken Heinz, Allan Chang, Gualtiero Nunz-Conti, Franco Cosi, Payal Singh, Tiziana Bond, "Versatile bio-organism detection using microspheres for future biodegradation and bioremediation studies," Proc. SPIE 11266, Laser Resonators, Microresonators, and Beam Control XXII, 112661E (2 March 2020);

[8] Hoang, Van Thuy & Stepniewski, Grzegorz & Czarnecka-Chrebelska, Karolina & Kasztelanic, Rafał & Van, Cao & Khoa, Dinh & Shao, Li-Yang & Smietana, Mateusz & Buczynski, Ryszard. (2019). Optical Properties of Buffers and Cell Culture Media for Optofluidic and Sensing Applications. Applied Sciences. 9. 1145. 10.3390/app9061145.

[9] Vollmer, F., & Arnold, S. (2008). Whispering-gallery-mode biosensing: label-free detection down to single molecules. Nature methods, 5(7), 591–596. https://doi.org/10.1038/nmeth.1221

[10] Vollmer, F., Braun, D., Libchaber, A., Khoshsima, M., Teraoka, I., & Arnold, S. (2002). Protein detection by optical shift of a resonant microcavity. Applied Physics Letters, 80(21), 4057-4059. https://doi.org/10.1063/1.1482797